

Bismuth gallate coordination networks inspired by an active
pharmaceutical ingredient

Supplementary Information

Erik Svensson Grape^a, Victoria Rooth^a, Simon Smolders^b, Sofia Takki^a, Ambre
Thiriez^c, Dirk De Vos^b, Tom Willhammar^a, A. Ken Inge^{*a}

^a. Department of Materials and Environmental Chemistry, Stockholm University, SE-106 91, Sweden

^b. Centre for Membrane Separations, Adsorption, Catalysis and Spectroscopy for Sustainable Solutions (cMACS),
Department of Microbial and Molecular Systems (M2S), KU Leuven, 3001 Leuven, Belgium

^c. Département Sciences et Génie Des Matériaux, INSA, Lyon 69621, France

Contents

1. Chemicals and Synthesis	
Chemical Reagents.....	S1
Synthesis of 1 _{MeOH} - Bi(C ₇ H ₃ O ₄).....	S1
Synthesis of 1 _{EtOH} - Bi(C ₇ H ₃ O ₄).....	S1
Synthesis of 2 - Bi(C ₇ H ₃ O ₄).....	S1
2. Structure Determination and Characterization	
Scanning electron microscopy (SEM).....	S2
3D electron diffraction (3D ED).....	S2-S4
Powder X-ray diffraction studies.....	S4-S7
Thermogravimetric analysis (TGA).....	S8-S9
FT-IR.....	S9
Variable temperature powder X-ray diffraction (VT-PXRD).....	S10-S11
Stability of 1 upon exposure to water.....	S11
3. Catalysis Experiments	
Synthesis of bismuth subgallate and bismuth ellagate (SU-101).....	S12
Procedure.....	S12
4. Supplemental References	S13

1. Chemicals and Synthesis

Chemical Reagents

The reagents were obtained as follows. Gallic acid monohydrate ($\geq 98\%$), bismuth nitrate pentahydrate (98%), and n-nonane ($\geq 99\%$) were purchased from Sigma Aldrich. Methanol ($\geq 99.8\%$) was purchased from Honeywell and VWR. Ethanol ($\geq 99.5\%$) was purchased from KilitoClean. Styrene oxide ($>97\%$) was purchased from Acros Organics. All chemicals were used as-received without further purification.

Synthesis of $1_{\text{MeOH}} - \text{Bi}(\text{C}_7\text{H}_3\text{O}_4)(\text{MeOH})$

In a typical synthesis, 50 mg of gallic acid monohydrate and 47 mg of bismuth nitrate pentahydrate were added to a 5 mL borosilicate 3.3 glass tube (Duran 12 x 100 mm, DWK Life Sciences) containing a PTFE-coated stir bar. Before sealing the container with a polybutylene terephthalate (PBT) cap containing a PTFE seal, 3 ml of methanol was added. The tube was then put into a pre-heated aluminium block kept at $120\text{ }^\circ\text{C}$ and stirred at 800 rpm for 2 hours. The tube was then allowed to cool down to room temperature outside the aluminium block, whereafter its contents were filtered off and left to dry under ambient conditions overnight. Yield: 28 mg (66 % of theoretical yield with respect to Bi^{3+}). The phase purity of the material was confirmed by PXRD and elemental analysis. Calculated (%) for $\text{Bi}(\text{C}_7\text{H}_3\text{O}_5)(\text{MeOH}) \cdot 0.5\text{MeOH}$: C 24.56 H 2.52; measured (%): C 23.50 H 2.24.

Synthesis of $1_{\text{EtOH}} - \text{Bi}(\text{C}_7\text{H}_3\text{O}_4)(\text{EtOH})$

In a typical synthesis, 50 mg of gallic acid monohydrate and 47 mg of bismuth nitrate pentahydrate were added to a 5 mL borosilicate 3.3 glass tube (Duran 12 x 100 mm, DWK Life Sciences) containing a PTFE-coated stir bar. Before sealing the container with a polybutylene terephthalate (PBT) cap containing a PTFE seal, 3 ml of ethanol was added. The tube was then put into a pre-heated aluminium block kept at $120\text{ }^\circ\text{C}$ and stirred at 800 rpm for 2 hours. The tube was then allowed to cool down to room temperature outside the aluminium block, whereafter its contents were filtered off and left to dry under ambient conditions overnight. Yield: 32 mg (78 % of theoretical yield with respect to Bi^{3+}). The phase purity of the material was confirmed by PXRD and elemental analysis. Calculated (%) for $\text{Bi}(\text{C}_7\text{H}_3\text{O}_5)(\text{EtOH}) \cdot 0.5\text{EtOH}$: C 26.98 H 2.72; measured (%): C 22.93 H 2.17.

Synthesis of $2 - \text{Bi}(\text{C}_7\text{H}_3\text{O}_4)$

In a typical synthesis, 50 mg of gallic acid monohydrate and 47 mg of bismuth nitrate pentahydrate were added to a 5 mL borosilicate 3.3 glass tube (Duran 12 x 100 mm, DWK Life Sciences) containing a PTFE-coated stir bar. Before sealing the container with a polybutylene terephthalate (PBT) cap containing a PTFE seal, 3 ml of methanol was added. The tube was then put into a pre-heated aluminium block kept at $120\text{ }^\circ\text{C}$ and stirred at 800 rpm for 6 hours. The tube was then allowed to cool down to room temperature outside the aluminium block, whereafter its contents were filtered off and left to dry under ambient conditions overnight. Yield: 35 mg (92 % of theoretical yield with respect to Bi^{3+}). The phase purity of the material was confirmed by PXRD and elemental analysis. Calculated (%) for $\text{Bi}(\text{C}_7\text{H}_3\text{O}_5) \cdot \text{MeOH}$: C 23.54 H 1.73; measured (%): C 24.62 H 1.61.

2. Structure Determination and Characterization

Scanning electron microscopy

Scanning electron microscopy (SEM) images were collected on a JEOL JSM7400F SEM.

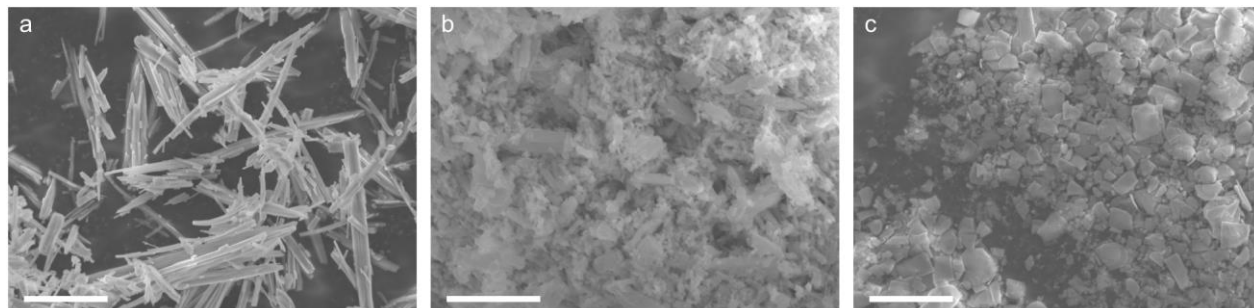


Fig. S1. SEM images of **1**_{MeOH} (a), **1**_{EtOH} (b), and **2** (c). Scale bar is equal to 5 μm .

3D electron diffraction (3DED)

Three-dimensional electron diffraction data were collected using a JEOL JEM2100 TEM, equipped with a Timepix detector from Amsterdam Scientific Instruments, while continuously rotating the crystal at $0.45^\circ \text{ s}^{-1}$. The experiment was carried out using Instamatic,¹ with data reduction performed in XDS.² e.s.d. values on unit cell parameters were estimated to be 0.5% of the unit cell lengths and 0.2° for the unit cell angles based on previous experiments performed on the same TEM.³ The merging of datasets was carried out using the XSCALE module of XDS, and the average unit cell parameters were used. The acquired intensities were then used to solve the structure of each phase using SHELXT,⁴ and refined using SHELXL,⁵ with electron scattering factors as previously published by Peng.⁶ From the 3DED data, all non-hydrogen atoms could be located in the initial structure solutions using the program SHELXT. Hydrogen atoms were placed and refined as part of a riding model. The refinement statistics for each phase are listed in the table that follows. Topological analyses of the materials were carried out using the software package ToposPro,⁷ as well as Systre,⁸ and 3dt (both part of the GAVROG package).⁹

Table S1. Crystallographic table of 3DED data and the refinement of **1**_{MeOH} (data merged from 7 crystals), **1**_{EtOH} (data merged from 4 crystals), **1**_{EtOH(stored)} (1 crystal) and **2** (1 crystal).

Compound	1 _{MeOH}	1 _{EtOH}	1 _{EtOH(stored)}	2
CCDC number	2183351	2183352	2183353	2183354
Empirical formula	C ₈ H ₇ BiO ₆	C ₉ H ₉ BiO ₆	C ₉ H ₉ BiO ₆	C ₇ H ₃ BiO ₅
Formula weight	408.12 g mol ⁻¹	422.14 g mol ⁻¹	422.14 g mol ⁻¹	376.08 g mol ⁻¹
Temperature	295(2) K	295(2) K	295(2) K	295(2) K
Wavelength	0.0251 Å	0.0251 Å	0.0251 Å	0.0251 Å
Crystal system	Orthorhombic	Orthorhombic	Orthorhombic	Monoclinic
Space group	<i>P</i> 2 ₁ 2 ₁ 2 ₁ (No. 19)	<i>P</i> 2 ₁ 2 ₁ 2 ₁ (No. 19)	<i>P</i> 2 ₁ 2 ₁ 2 ₁ (No. 19)	<i>P</i> 2 ₁ / <i>c</i> (No. 14)
Unit cell dimensions	<i>a</i> = 7.62(4) Å <i>b</i> = 8.38(4) Å <i>c</i> = 16.68(8) Å	<i>a</i> = 7.89(4) Å <i>b</i> = 8.61(4) Å <i>c</i> = 17.38(9) Å	<i>a</i> = 7.73(4) Å <i>b</i> = 6.84(3) Å <i>c</i> = 16.87(8) Å	<i>a</i> = 11.75(6) Å <i>b</i> = 7.64(4) Å <i>c</i> = 10.11(5) Å <i>β</i> = 104.8(2)°
Volume	1066(9) Å ³	1181(10) Å ³	891(8) Å ³	878(8) Å ³
Z	4	4	4	4
Density (calc.)	2.254 g cm ⁻³	2.375 g cm ⁻³	3.147 g cm ⁻³	2.846 g cm ⁻³
Index ranges	-9 ≤ <i>h</i> ≤ 9 -10 ≤ <i>k</i> ≤ 10 -21 ≤ <i>l</i> ≤ 21	-9 ≤ <i>h</i> ≤ 9 -10 ≤ <i>k</i> ≤ 10 -21 ≤ <i>l</i> ≤ 21	-9 ≤ <i>h</i> ≤ 9 -6 ≤ <i>k</i> ≤ 6 -20 ≤ <i>l</i> ≤ 20	-14 ≤ <i>h</i> ≤ 14 -9 ≤ <i>k</i> ≤ 9 -12 ≤ <i>l</i> ≤ 12
Reflections collected	25993	16554	3234	7034
Completeness	98.1 % (0.73 Å)	99.8 % (0.80 Å)	72.9 % (0.80 Å)	89.7 % (0.81 Å)
Independent reflections	2222 [R(int) = 0.2958]	2396 [R(int) = 0.2110]	1278 [R(int) = 0.1407]	1590 [R(int) = 0.2322]
Data / restr. / param.	2222/208/139	2396/168/147	1278/54/66	1590/176/119
Goodness-of-fit on F ²	1.181	1.250	0.917	1.138
Final R index [<i>I</i> > 4σ(<i>I</i>)]	R1 = 0.1399	R1 = 0.1409	R1 = 0.3069	R1 = 0.2043

Powder X-Ray diffraction studies

In-house PXRD measurements were carried out using a Panalytical X'pert Pro diffractometer (Cu K α 1,2, $\lambda_1 = 1.540598 \text{ \AA}$, $\lambda_2 = 1.544426 \text{ \AA}$) using a Bragg–Brentano geometry, loading the samples on zero-background Si plates. Pawley refinements against PXRD data were carried out in TOPAS-Academic V6.¹⁰

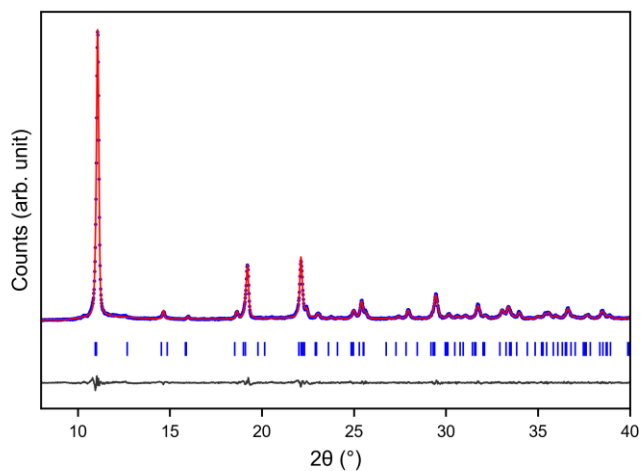


Fig. S2. Plot for the Pawley refinement of **1**_{MeOH}. The data were collected using Cu K α radiation ($\lambda_1 = 1.540598 \text{ \AA}$, $\lambda_2 = 1.544426 \text{ \AA}$).

Table S2. Crystallographic table for the Pawley refinement of **1**_{MeOH} against PXRD data.

Compound	1 _{MeOH}
Crystal system	Orthorhombic
Space group	<i>P</i> 2 ₁ 2 ₁ 2 ₁ (No. 19)
Unit cell dimensions	$a = 7.740(1) \text{ \AA}$ $b = 9.3402(9) \text{ \AA}$ $c = 16.054(1) \text{ \AA}$
Volume (\AA^3)	1160.7(3) \AA^3
Wavelength	$\lambda_1 = 1.540598 \text{ \AA}$ $\lambda_2 = 1.544426 \text{ \AA}$
Refinement method	Pawley
Refinement statistics	$R_{wp} = 8.30 \%$ GOF = 1.30

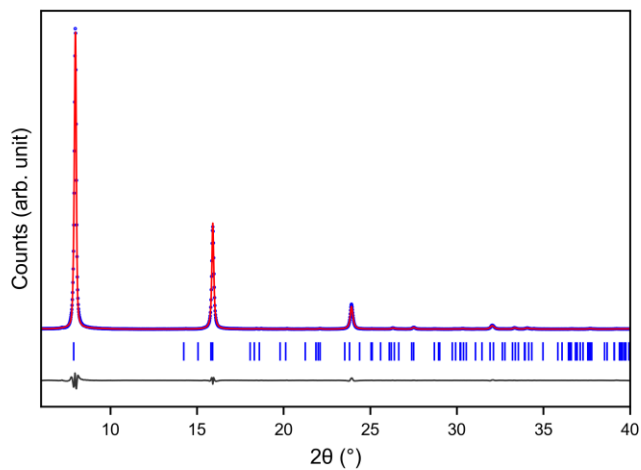


Fig. S3. Plot for the Pawley refinement of **2**. The data were collected using Cu K α radiation ($\lambda_1 = 1.540598 \text{ \AA}$, $\lambda_2 = 1.544426 \text{ \AA}$).

Table S3. Crystallographic table for the Pawley refinement of **2** against PXRD data.

Compound	2
Crystal system	Monoclinic
Space group	$P2_1/c$ (No. 14)
Unit cell dimensions	$a = 11.568(3) \text{ \AA}$ $b = 7.444(2) \text{ \AA}$ $c = 10.407(9) \text{ \AA}$ $\beta = 104.37(5)^\circ$
Volume (\AA^3)	$868.2(9) \text{ \AA}^3$
Wavelength	$\lambda_1 = 1.540598 \text{ \AA}$ $\lambda_2 = 1.544426 \text{ \AA}$
Refinement method	Pawley
Refinement statistics	$R_{\text{wp}} = 9.82 \%$ GOF = 3.65

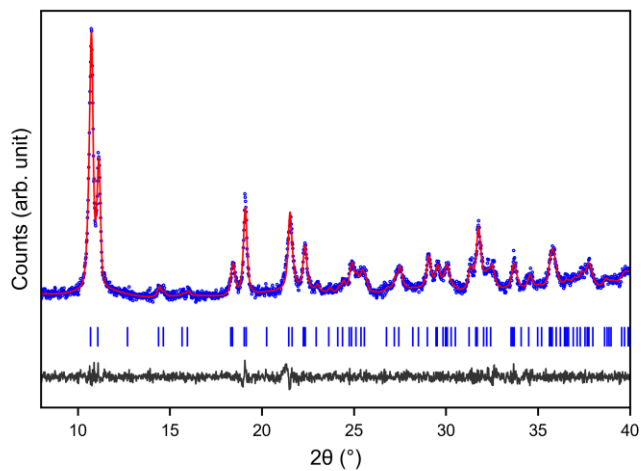


Fig. S4. Plot for the Pawley refinement of **1EtOH**. The data were collected using Cu K α radiation ($\lambda_1 = 1.540598 \text{ \AA}$, $\lambda_2 = 1.544426 \text{ \AA}$).

Table S4. Crystallographic table for the Pawley refinement of **1EtOH** against PXRD data.

Compound	1EtOH
Crystal system	Orthorhombic
Space group	<i>P</i> 2 ₁ 2 ₁ 2 ₁ (No. 19)
Unit cell dimensions	<i>a</i> = 7.742(3) \AA <i>b</i> = 9.680(2) \AA <i>c</i> = 15.945(3) \AA
Volume (\AA^3)	1194.9(6) \AA^3
Wavelength	$\lambda_1 = 1.540598 \text{ \AA}$ $\lambda_2 = 1.544426 \text{ \AA}$
Refinement method	Pawley
Refinement statistics	$R_{\text{wp}} = 5.81 \%$ GOF = 0.92

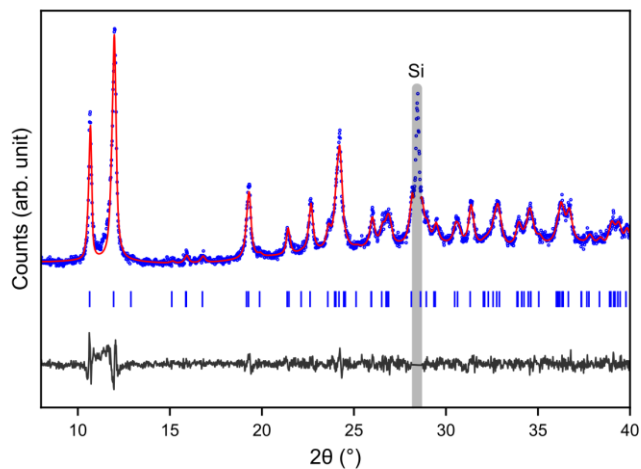


Fig. S5. Plot for the Pawley refinement of $1E_{10}H$ after being exposed to a reduced pressure environment (1 mbar, room temperature). The data were collected using Cu K α radiation ($\lambda_1 = 1.540598 \text{ \AA}$, $\lambda_2 = 1.544426 \text{ \AA}$). The grey area denotes to peak position of the $\langle 111 \rangle$ peak of Si, which was used as an internal standard for the VT-PXRD measurements.

Table S5. Crystallographic table for the Pawley refinement of $1E_{10}H$, after being exposed to a reduced pressure environment (1 mbar) at room temperature.

Compound	$1E_{10}H$ (vac, RT)
Crystal system	Orthorhombic
Space group	$P2_12_12_1$ (No. 19)
Unit cell dimensions	$a = 7.540(2) \text{ \AA}$ $b = 8.271(3) \text{ \AA}$ $c = 16.616(4) \text{ \AA}$
Volume (\AA^3)	$1036.2(5) \text{ \AA}^3$
Wavelength	$\lambda_1 = 1.540598 \text{ \AA}$ $\lambda_2 = 1.544426 \text{ \AA}$
Refinement method	Pawley
Refinement statistics	$R_{wp} = 9.81 \%$ GOF = 1.16

Thermogravimetric analysis (TGA)

Thermogravimetric analysis data were gathered using a TA Instruments Discovery TGA, in air using a heating rate of 10 degrees per minute. The sum formula best matching the observed TGA data and CHN analysis results of **1**_{MeOH} was determined to be $\text{Bi}(\text{C}_7\text{H}_3\text{O}_5)(\text{MeOH}) \cdot \text{MeOH}$ and for **1**_{EtOH} a sum formula of $\text{Bi}(\text{C}_7\text{H}_3\text{O}_5)(\text{EtOH}) \cdot 0.5\text{EtOH}$. As can be seen in the TGA plots, mass loss is immediately observed indicating the solvent in the pores is readily lost even under ambient conditions. For **2**, the best match is a sum formula of $\text{Bi}(\text{C}_7\text{H}_3\text{O}_5) \cdot 0.5\text{MeOH}$.

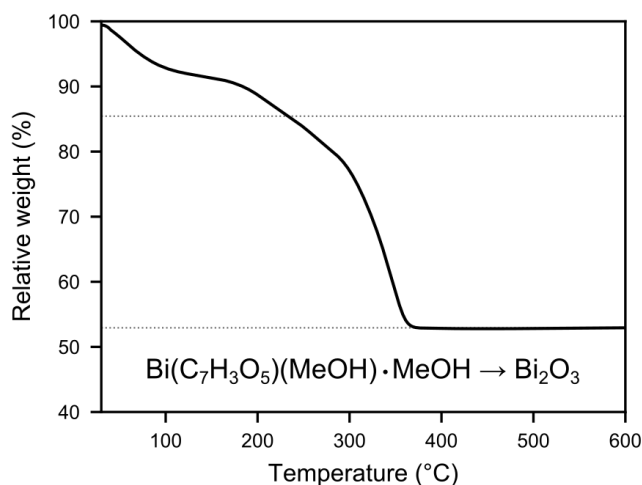


Fig. S6. Thermogravimetric analysis of **1**_{MeOH} in air. The dashed lines indicated expected relative mass remaining after loss of MeOH and gallate, assuming an initial formula of $\text{Bi}(\text{C}_7\text{H}_3\text{O}_5)(\text{MeOH}) \cdot \text{MeOH}$, which is then converted into Bi_2O_3 when heated beyond 350 °C.

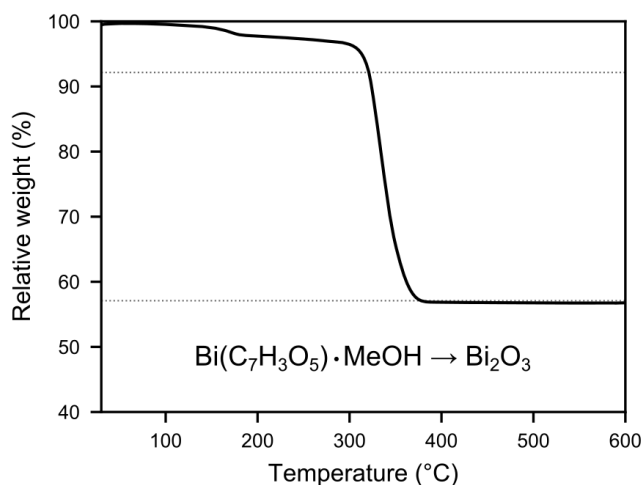


Fig. S7. Thermogravimetric analysis of **2** in air. The dashed lines indicated expected relative mass remaining after loss of MeOH and gallate, assuming an initial formula of $\text{Bi}(\text{C}_7\text{H}_3\text{O}_5) \cdot \text{MeOH}$, which is then converted into Bi_2O_3 when heated beyond 350 °C.

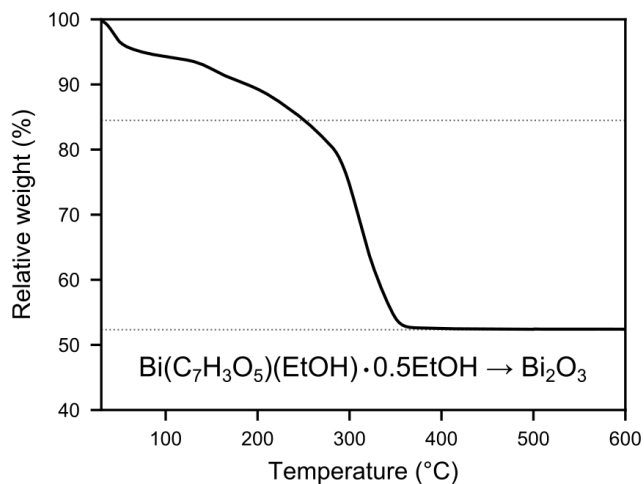


Fig. S8. Thermogravimetric analysis of **1_{EtOH}** in air. The dashed lines indicated expected relative mass remaining after loss of EtOH and gallate, assuming an initial formula of $\text{Bi}(\text{C}_7\text{H}_3\text{O}_5)(\text{EtOH}) \cdot 0.5\text{EtOH}$, which is then converted into Bi_2O_3 when heated beyond 350 °C.

FT-IR Spectroscopy

Spectra were recorded on a Varian 670-IR spectrometer equipped with a Specac Golden Gate™ ATR setup.

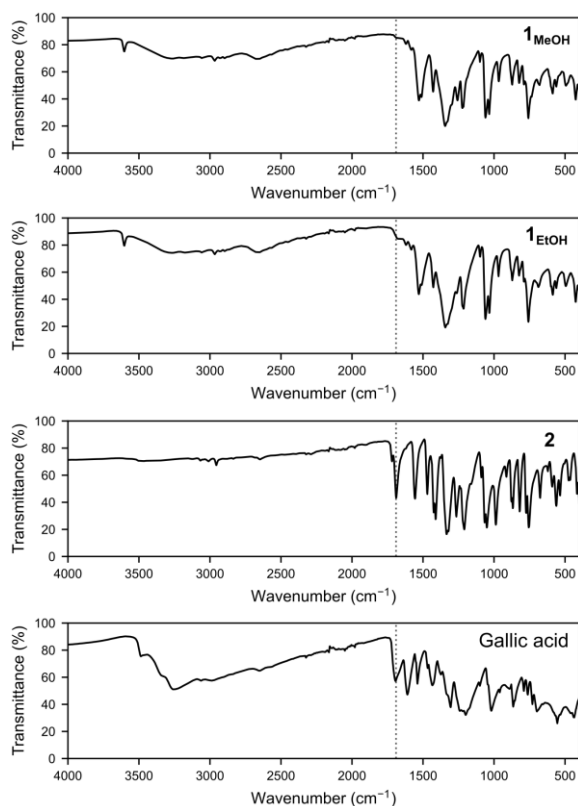


Fig. S9. FT-IR spectra of as-synthesized **1_{MeOH}**, **1_{EtOH}**, **2**, and gallic acid. The dashed line is drawn at 1690 cm^{-1} , indicating the presence of a protonated carboxylic acid.

Variable temperature powder X-ray diffraction (VT-PXRD)

Thermodiffraction measurements were carried out using the aforementioned in-house diffractometer, equipped with an Anton Paar XRK 900 high-temperature chamber.

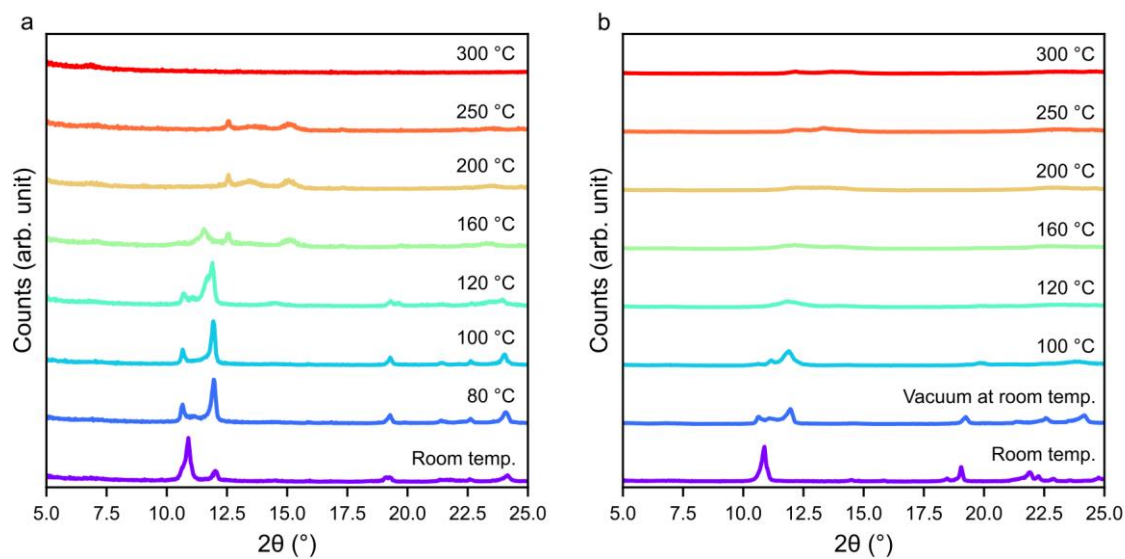


Fig. S10. Variable temperature diffraction data for **1**_{MeOH} (a) in air and (b) under vacuum.

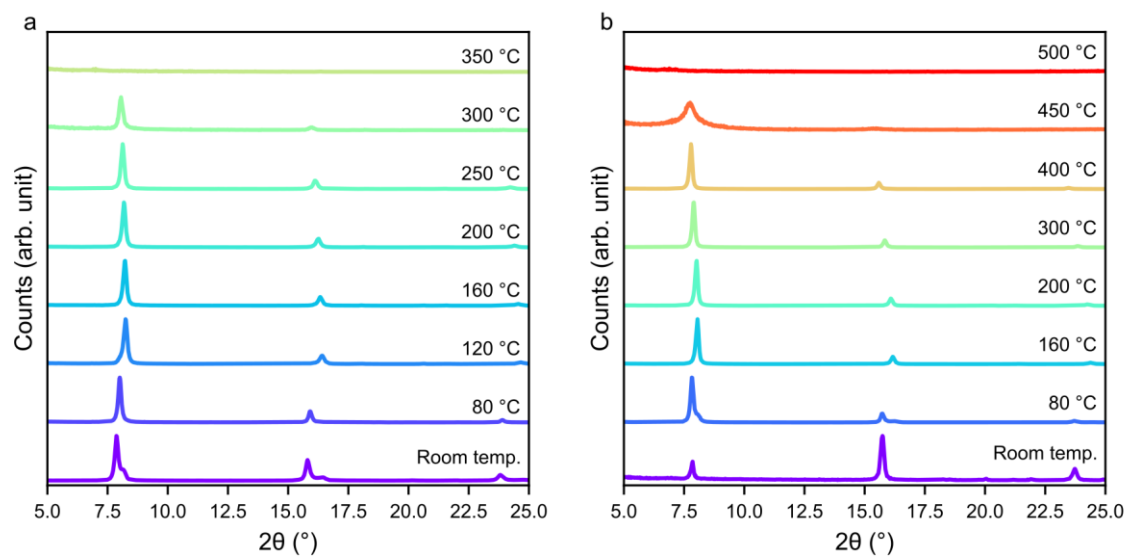


Fig. S11. Variable temperature diffraction data for **2** (a) in air and (b) under vacuum.

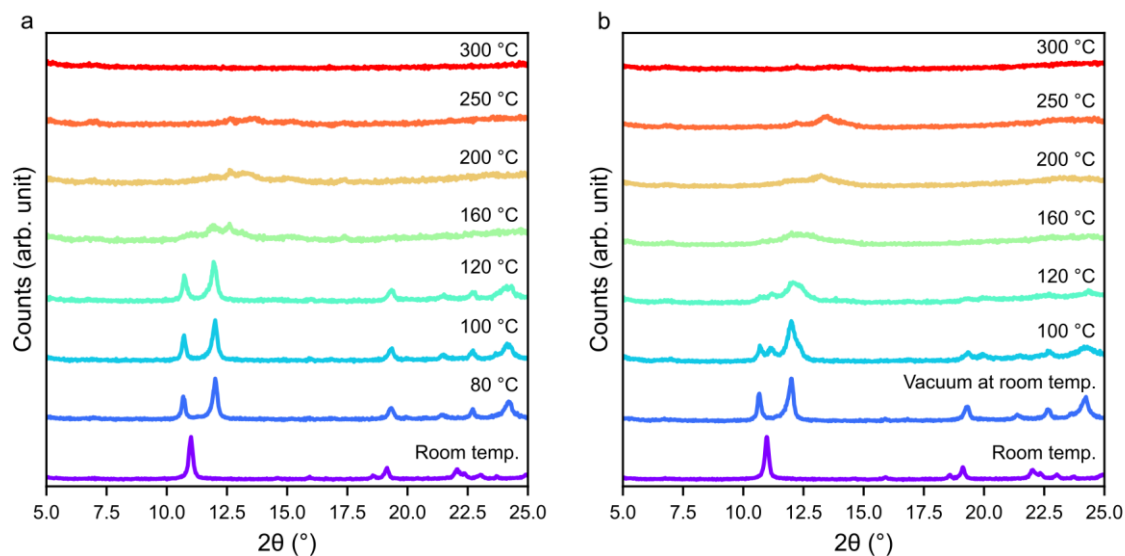


Fig. S12. Variable temperature diffraction data for 1_{EtOH} (a) in air and (b) under vacuum.

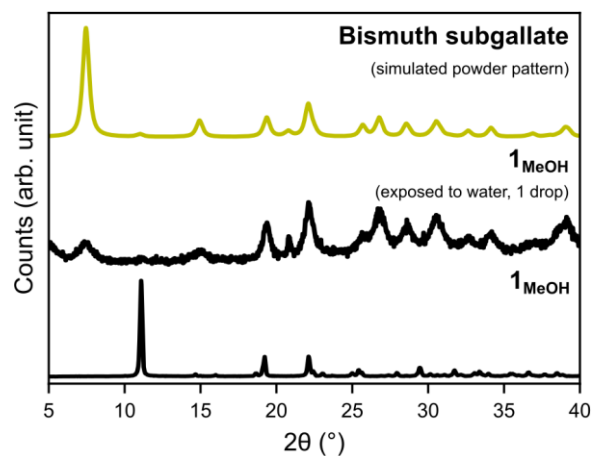


Fig. S13. Measured PXRD patterns for as-synthesized 1_{MeOH} (bottom), the same sample of 1_{MeOH} after allowed to dry in one drop of water (middle), converting into bismuth subgallate, and simulated powder pattern of bismuth subgallate (top, using the CIF available in the Cambridge Structural Database - CCDC 1526756).

3. Catalysis experiments

Synthesis of bismuth subgallate and bismuth ellagate (SU-101)

Fine powders of bismuth subgallate and the bismuth ellagate MOF named SU-101 were prepared according to published procedures.^{11,12} Both materials were used without any further purification.

Procedure

The catalysis trials were carried in 2 ml crimp cap vials, to which 25 mg of each bismuth-based material was added (**2**, BSG, and SU-101), along with a PTFE-coated stir bar. The open containers were then put in a preheated circulation oven at 110 °C overnight, after which they were removed and reweighed. A reaction mixture was then prepared, composed of 40 mg ml⁻¹ of styrene oxide in methanol, as well as 40 mg ml⁻¹ of nonane as an internal standard, which was added as to each container as to give a 10:1 molar ratio between styrene oxide and Bi³⁺ for each solid. After addition of the reaction mixture, the vials were sealed and put in a pre-heated aluminium heating block at 40 °C. Aliquots of 100 µl were then taken and filtered off after 10 and 30 minutes, as well as after 1, 2, 6 and 24 hours. Gas chromatograms were acquired using a Shimadzu GC-2010 gas chromatograph equipped with a 60 m CP-Sil-5 column, and were analysed using the Shimadzu LabSolutions software package. Product formation was further verified by GC-MS measurements using an Agilent 6890 chromatograph with a HP-5MS column and a mass chromatograph equipped with a 5973 MSD detector. The filter test was executed analogously but the hot reaction mixture was filtered after 30 minutes and transferred (while still hot) to another crimp cap vial, after which reaction was allowed to proceed at 40 °C.

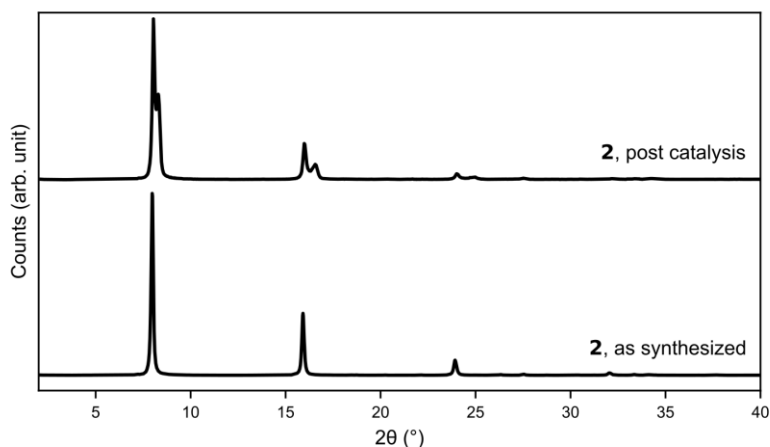


Fig. S14. Comparison of PXRD patterns of **2** before (bottom) and after (top) catalysis experiments. The splitting of intense peaks can be attributed to a shift in the interlayer distance of the structure and is also observed for the VT-PXRD data (Figure S11).

Supplemental references

- 1 M. O. Cichocka, J. Ångström, B. Wang, X. Zou and S. Smeets, *J. Appl. Crystallogr.*, 2018, **51**, 1652–1661.
- 2 W. Kabsch, *Acta Crystallogr. Sect. D Biol. Crystallogr.*, 2010, **66**, 125–132.
- 3 S. Smeets, S. I. Zones, D. Xie, L. Palatinus, J. Pascual, S. J. Hwang, J. E. Schmidt and L. B. McCusker, *Angew. Chemie - Int. Ed.*, 2019, **58**, 13080–13086.
- 4 G. M. Sheldrick, *Acta Crystallogr. Sect. A Found. Crystallogr.*, 2015, **71**, 3–8.
- 5 G. M. Sheldrick, *Acta Crystallogr. Sect. A Found. Crystallogr.*, 2008, **64**, 112–122.
- 6 L. M. Peng, *Micron*, 1999, **30**, 625–648.
- 7 V. A. Blatov, A. P. Shevchenko and D. M. Proserpio, *Cryst. Growth Des.*, 2014, **14**, 3576–3586.
- 8 O. Delgado-Friedrichs and M. O’Keeffe, *Acta Crystallogr. Sect. A Found. Crystallogr.*, 2003, **59**, 351–360.
- 9 O. Delgado-Friedrichs, The GAVROG Project, <http://www.gavrog.org/>.
- 10 A. A. Coelho, *J. Appl. Crystallogr.*, 2018, **51**, 210–218.
- 11 Y. Wang, S. Takki, O. Cheung, H. Xu, W. Wan, L. Öhrström and A. K. Inge, *Chem. Commun.*, 2017, **53**, 7018–7021.
- 12 E. Svensson Grape, J. Gabriel Flores, T. Hidalgo, E. Martínez-Ahumada, A. Gutierrez-Alejandre, A. Hautier, D. R. Williams, M. O’Keeffe, L. Öhrström, T. Willhammar, P. Horcajada, I. A. Ibarra and A. Ken Inge, *J. Am. Chem. Soc.*, 2020, **142**, 16795–16804.